ARTICLE

Reversal of cardiac, vascular, and renal dysfunction by non-quinazoline α1-adrenolytics in DOCA-salt hypertensive rats: a comparison with prazosin, a quinazoline-based α1-adrenoceptor antagonist

Monika Kubacka[1] · Monika Zadrożna[2] · Barbara Nowak[2] · Magdalena Kotańska[1] · Barbara Filipek[1] ·
Anna Maria Waszkielewicz[3] · Henryk Marona[3] · Szczepan Mogilski[1]

Abstract

We investigated the therapeutic effect of **MH-76** and **MH-79**, which are non-quinazoline α1-adrenoceptor antagonists with an additional ability to stimulate the nitric oxide (NO)/cyclic guanosine monophosphate (cGMP)/K + pathway, on deoxycorticosterone acetate (DOCA)-salt induced hypertension in rats. Prazosin was used as a reference compound, as quinazoline-based α1-adrenolytics may potentially exert unfavorable proapoptotic and necrotic effects. DOCA-salt hypertension was induced by DOCA (20 mg/kg s.c., twice weekly) administration plus 1% NaCl and 0.2% KCl solutions in drinking water for 12 weeks. The studied compounds **MH-76**, **MH-79** (10 mg/kg i.p.) or prazosin (0.4 mg/kg i.p.) were administered to the DOCA-salt-treated rats, starting from the 6th week of DOCA-salt treatment and continuing for 6 weeks. This study showed that the administration of **MH-79** and, to a lesser extent, **MH-76** decreased elevated systolic blood pressure and heart rate, reduced heart and kidney hypertrophy, and reversed the histopathological alterations of the heart, kidney, and vessels in DOCA-salt hypertensive rats. **MH-79** reversed endothelial dysfunction, which reduced inflammatory cell infiltration, arteriosclerotic alterations in renal and coronary arteries, and tubulointerstitial fibrosis. Prazosin showed a potent hemodynamic effect and reduced cardiac and renal fibrosis but exerted detrimental effects on blood vessels, potentiating fibroplasia of the media of the intrarenal artery and causing calcification of coronary arteries. Prazosin did not reverse endothelial dysfunction. Our results show the beneficial effect of non-quinazoline α1-adrenolytics on cardiac, vascular, and renal dysfunction in DOCA-salt hypertensive rats. Our findings also support the idea that targeting endothelial protection and endothelial integrity would yield beneficial effects against cardiac, blood vessel and renal injury related to hypertension.

✉ Monika Kubacka
mfkuback@cyf-kr.edu.pl

1 Faculty of Pharmacy, Department of Pharmacodynamics, Medical College, Jagiellonian University, Medyczna 9, 30-688 Kraków, Poland

2 Faculty of Pharmacy, Department of Cytobiology, Medical College, Jagiellonian University, Medyczna 9, 30-688 Kraków, Poland

3 Faculty of Pharmacy, Chair of Organic Chemistry, Department of Bioorganic Chemistry, Medical College, Jagiellonian University, Medyczna 9, 30-688 Kraków, Poland

Introduction

Hypertension is an important risk factor for cardiovascular diseases, and its treatment reduces cardiovascular morbidity and mortality [1]. Human and animal studies indicate that among other factors, an overactive sympathetic nervous system significantly contributes to the development of hypertension [2]. For several years, α1-adrenolytics have been used in the treatment of hypertension; they exert, in addition to lowering blood pressure, a number of other beneficial effects (e.g., improvement of fibrinolysis and reduction of platelet aggregation) and have been shown, unlike many other antihypertensives, to have a low incidence of sexual dysfunction and favorable effects on

metabolic profiles [1, 3, 4]. However, in the Anti-hypertensive and Lipid-Lowering Treatment to Prevent Heart Attack Trial (ALLHAT), the α1-adrenoceptor antagonist doxazosin was associated with a higher risk of combined cardiovascular disease events, particularly congestive heart failure [3–6]. A possible explanation for the ALLHAT results may be the observation that doxazosin and other quinazoline-based α1-adrenolytics induce apoptosis and necrosis in cultured human and murine cardiomyocytes, as well as coronary smooth muscle cell cycle arrest [4, 6, 7]. This finding may explain the ALLHAT outcome because cell death occurs in myocardial dysfunction and contributes to heart failure [4, 6]. However, these effects are independent of α1-adrenoceptor blockade and are probably connected with the presence of a quinazoline moiety in prazosin and doxazosin molecules [4, 7]. Recent studies have shown that quinazoline-based α1-adrenoceptor antagonists induce the apoptosis of other cell types, including prostate cells, through an alternative mechanism unrelated to α1-adrenoceptors [7, 8]. These compounds are currently used rather in the treatment of benign prostatic hypertrophy than cardiovascular diseases, and they are under investigation as potential anticancer drugs [7–9]. On the other hand, fibrosis, necrosis, or apoptosis induction was never shown for non-quinazoline-based α1-adrenolytics: phenoxybenzamine [4, 6, 7], urapidil, a 1-(2-methoxyphenyl)piperazine derivative [10], or tamsulosin—a sulfonamide derivative [7].

In our previous work, we described the synthesis of newly designed 1-(2-methoxyphenyl)piperazine derivatives, which displayed high affinity for α1-adrenoceptors [11]. Among the achieved derivatives, **MH-76** (1-[(2,6-dimethylphenoxy)propyl]-4-(2-methoxyphenyl)piperazine hydrochloride) and **MH-79** (1-[(2-chlor-6-methylphenoxy)propyl]-4-(2-methoxyphenyl)piperazine hydrochloride), (Supplementary Figure 1) exhibited the most favorable α1-adrenoceptor blocking properties. These non-quinazoline α1-adrenolytics may be regarded as structural urapidil analogs. In addition, **MH-76** and **MH-79** showed significant hypotensive activity, stronger than that of urapidil [12]. Moreover, **MH-76** and **MH-79** possess some additional pleiotropic features as they also activate the endothelial nitric oxide (NO)-cyclic guanosine monophosphate (cGMP) signaling pathway [13].

The aim of the present study was to investigate the therapeutic effect of **MH-76** and **MH-79** on deoxycorticosterone acetate (DOCA)-salt induced hypertension in rats (with administration of compounds starting 6 weeks after initiation of DOCA-salt hypertension), which is an established model of severe hypertension with renal dysfunction [14]. The damage to target organs (heart, kidney, and vessels) induced by DOCA and salt overload resembles complications observed in patients with hypertension and heart failure [15]. In this study, we determined whether long-term use of **MH-76** and **MH-79**

may treat hemodynamic disturbances in DOCA-salt hypertensive rats and whether **MH-76** and **MH-79** are able to reduce or reverse hypertension-induced complications such as endothelial dysfunction, cardiac remodeling, and renal dysfunction. It was of particular interest to compare the effects of prazosin, a quinazoline derivative, and tested compounds, namely, non-quinazoline α1-adrenolytics, to evaluate the involvement of α1-adrenoceptor blockade in cardiovascular and renal function.

Methods

Animals

Experiments were carried out using male Wistar rats (Krf: (WI) WU), 180–200 g, age 7 weeks. The animals were housed in constant temperature facilities exposed to 12:12 h light/dark cycles and were maintained on a standard pellet diet. All procedures were conducted according to the guidelines of the National Research Council and approved by the Local Ethics Committee on Animal Experimentation (resolution no. 148/2015, 24.06.2015) in Krakow, Poland. The rats were acclimated to handling.

Experimental protocol

Hypertension in rats was induced by administering DOCA and salt solution for 12 weeks [16]. DOCA-treated animals (20 mg/kg s.c., twice weekly, dissolved in olive oil) were administered 1% NaCl and 0.2% KCl solutions instead of drinking water, whereas the control group was maintained on normal drinking water. To study the therapeutic effects of the test compounds, they were administered for the last 6 weeks in DOCA-salt-treated animals. Prazosin was used as a reference compound. The test compounds were administered at a dose of 10 mg/kg i.p. daily. This dose was chosen on the basis of our previous research, both published [12] and unpublished, as an effective and well-tolerated dose.

In total, 40 male Wistar rats were divided into the following 5 groups ($n = 8$):

Group 1: Control group. Animals were administered olive oil (1 ml/kg s.c., twice weekly) and saline (1 ml/kg i.p. daily) for the last 6 weeks.

Group 2—DOCA-salt group. Animals were administered DOCA (20 mg/kg s.c., twice weekly) for 12 weeks. Drinking water was replaced with a solution of 1% NaCl and 0.2% KCl. Animals received saline (1 ml/kg i.p. daily) for the last 6 weeks of DOCA-salt treatment.

Group 3—DOCA-salt + MH-76. Animals were administered DOCA (20 mg/kg s.c., twice weekly) for 12 weeks. Drinking water was replaced with a solution of 1% NaCl and 0.2% KCl. MH-76 (10 mg/kg i.p. daily) was

administered to the DOCA-salt-treated rats for the last 6 weeks of DOCA-salt treatment.

Group 4—DOCA-salt + MH-79. Animals were administered DOCA (20 mg/kg s.c., twice weekly) for 12 weeks. Drinking water was replaced with a solution of 1% NaCl and 0.2% KCl. MH-79 (10 mg/kg i.p. daily) was administered to the DOCA-salt-treated rats for the last 6 weeks of DOCA-salt treatment.

Group 5—DOCA-salt + prazosin. Animals were administered DOCA (20 mg/kg s.c., twice weekly) for 12 weeks. Drinking water was replaced with a solution of 1% NaCl and 0.2% KCl. Prazosin (0.4 mg/kg i.p. daily) was administered to the DOCA-salt-treated rats for the last 6 weeks of DOCA-salt treatment.

At the end of the experiment, all rats were anesthetized with thiopental (75 mg/kg i.p.), and blood was collected. Within 30 s after collection, the blood was centrifuged for 10 min at 3000 rpm, and all samples were stored at −80 °C until they were assayed. The heart and right kidney were excised for histological evaluation. Body weight, heart weight, and kidney weight were also measured at the end of the study. Furthermore, from each animal, a segment of the thoracic aorta was rapidly removed for evaluation of the endothelial vasodilator function (relaxant effect of carbachol).

Measurement of systolic blood pressure

The systolic blood pressure and heart rate were measured in weeks 0 and 1–12 at the same time of the day. A non-invasive tail cuff system (ADInstruments, PowerLab Data Acquisition System, United Kingdom) was used.

Biochemical assays

The concentrations of creatinine, urea, norepinephrine, C-reactive protein (CRP, serum), and interleukin 6 (IL-6, kidney) were determined with the use of commercially available kits (SunRed Bio, Fine Test Biotech).

Measurements of antioxidant activity

Preparation of tissue homogenates

The frozen kidneys were weighed, and homogenates were prepared by homogenization of 1 g of the tissue in 4 ml of 0.1 M phosphate buffer, pH 7,4 using an IKA-ULTRA-TURRAX T8 homogenizer. Kidney homogenates were next used for assays of malondialdehyde and nonprotein thiol levels.

Determination of lipid peroxidation

The level of malondialdehyde (MDA) as an indicator of lipid peroxidation was estimated based on the level of thiobarbituric acid reactive substances (TBA) using the TBA spectrophotometric assay as described earlier [17].

Determination of nonprotein sulfhydryl group (NPSH) level

In addition, kidney homogenates were used for an assay of the NPSH level [17]. The level of NPSH was estimated according to the method described by Sedlak and Lindsay [18]. The total content of nonprotein sulfhydryl groups was determined from a standard curve for 1 mM glutathione.

Functional studies

Segments of thoracic aorta were placed in a Krebs–Henseleit solution and suspended in organ bath chambers (20 ml) and attached to an isometric force displacement transducer (FDT10-A. BIOPAC Systems, Inc., COMMAT, Ltd., Turkey and 720MO, DMT, Denmark). All rings were gradually stretched to a basal resting tension of 2 g, and the preparations were allowed to equilibrate for 45 min. After the equilibration period, the aortic rings were contracted by phenylephrine (3 μM), and when the contractile response was stabilized, the endothelial-dependent relaxation was evaluated by cumulative addition of carbachol (from 10^{-9} to 10^{-4} mol/l).

Histopathological analysis

Cardiac and renal tissue samples were fixed in 10% buffered formaldehyde and then processed, embedded in paraffin and sectioned (3 μm and 5 μm). Longitudinal kidney and heart sections were stained with Masson's trichrome, picrosirius red, periodic acid-Schiff (PAS), von Koss and May-Grunwald Giemsa, following standard techniques. The morphological studies were performed by a pathologist in blinded randomized sections of the tissues, with a light microscope (Olympus BX41, Japan) and using the most appropriate staining for each lesion. The histomorphometric measurements were performed with computerized imaging CellSens Dimension (Olympus) software. Digital images were taken using a computerized digital camera (Olympus UC90, Olympus).

Left ventricular wall thickness and cardiac/renal arterial parameters

In the heart, different parameters of cardiovascular injury were analyzed in (three) longitudinal sections at different levels of the left ventricle. The left ventricular wall thickness was assessed in the middle central region of the cardiac cavities.

Hyaline arteriopathy Cardiac arteriolar hyalinosis was semiquantitatively assessed as follows: grade 0, no

hyalinosis of the vessel wall; grade 1, hyalinosis of less than one-quarter of arterioles; grade 2, hyalinosis of one-quarter to one-half of arterioles; and grade 3, hyalinosis involving more than one-half of arterioles.

Cardiac and renal arterial parameters of arteriosclerotic lesions were examined by a semiquantitative scale as follows: grade 0, no changes; grade 1, mild changes; grade 2, moderate lesion; and grade 3, severe lesion (with definite atherosclerotic plaque formation).

The analysis of cardiac arteriosclerotic lesions involved 1. foam cell abundance (transformed either from macrophages or from smooth muscle cells—without distinction), 2. vascular and perivascular fibrosis, and 3. immune/inflammatory cell accumulation in the perivascular area. The mean calculated from the independently assessed value of the three parameters is presented as a cardiac arteriosclerotic index. The analysis of coronary atherosclerotic lesions involved changes closest to the tunica intima and was scored as the summation of 1. macrophage infiltration, 2. foam cell occurrence, 3. intracellular and extracellular lipid formation, 4. smooth muscle cell migration, 5. epithelial cell transformation, and 6. damage to the tunica intima. The mean calculated from the independently assessed value of the six parameters is presented as a coronary atherosclerotic index.

Renal atherosclerosis The analysis of principal branches of the renal artery included the severity of microscopic alteration of individual processes implicated in atherosclerotic plaque formation, even if the phenomena occurred independently of each other (Masson's trichrome staining sections). The range of most distinguishing processes involved leukocyte (monocyte) cumulation and adhesion to the endothelium, immune cell migration into the sub-endothelium, endothelial dysfunction (with immune cell extravasation), inflammatory cell accumulation within the tunica intima, occurrence of foam cells filled with intracellular fat, fatty streak occurrence, fibrous cap formation, and internal elastic lamina fenestration.

An uninfluenced assessment for fibromuscular alteration of the tunica media of the intrarenal principal branches of artery (PAS) was performed. The parameter was evaluated qualitatively by stereometric analysis. A two-dimensional stereometric grid, namely, the CellSens Dimension (Olympus) software tool, was used, in which the measurement surface was represented as a set of coordinates of grid points and then calculated as a percentage.

Arterial calcification The cardiac arteries of the left ventricle were analyzed in paraffin sections stained with Von Kossa for calcium deposition. Calcification was examined by using a semiquantitative scale as follows: grade 0, no calcinosis present in the arterial wall; grade 1, mild calcinosis in the wall of 1–2 arteries per section; grade 2, moderate calcinosis in the wall of 3-4 arteries per section; and grade 3, severe calcinosis in the wall of >5 arteries per section.

The left ventricle and kidney sclerosis The percentage of myocardial interstitial fibrosis visualized by picrosirius red staining was measured on 10 randomly selected microscopic fields of the left ventricular sections (×100 magnification) using the two-dimensional stereometric grid (the CellSens Dimension (Olympus) software).

Sections of kidneys were examined for the level of glomerular and tubulointerstitial sclerosis using the 0 to 4 injury scale. For glomeruli, the sclerotic index was calculated as the percentage of glomeruli with fibrosis (picrosirius red staining), hyalinosis, or leukocytes (PAS staining), as follows: grade 0, no glomeruli with deposition; grade 1, <25%; grade 2, 25–50%; grade 3, 51–75%; and grade 4, 76–100%. At least 200 glomeruli were scored to estimate the sclerotic index of a rat. The analysis of tubulointerstitial injury was carried out in picrosirius red and PAS-stained sections. From each kidney, longitudinal sections of cortical areas (1 mm^2, ×100 magnification) were analyzed. The analysis included fibrosis, tubular dilatation with cast formation, thickening of the tubular membrane, and focal tubular atrophy. To obtain the tubulointerstitial sclerosis index, we used the following scoring system: grade 0, no tubulointerstitial injury; grade 1, <25% of the tubulointerstitium injured; grade 2, 25–50% of the tubulointerstitium injured; grade 3, 51–75% of the tubulointerstitium injured; and grade 4, >75% of the tubulointerstitium injured. Data are presented as the mean value of the four tubulointerstitial injury parameters.

The left ventricle and renal infiltration by leukocytes The May–Grunwald Giemsa and PAS-stained myocardial and renal tissues were analyzed for infiltration by leukocytes: lymphocytes, macrophages, neutrophils, eosinophils, and mast cells. The whole longitudinal kidney cross-sections and left ventricular sections were analyzed in high-power field images (×200 magnification) using an Olympus BX41 microscope and the computerized imaging CellSens Dimension software. For myocardial sections, only mast cells were found and presented as the mean numerical density per 0.1 mm^2 of the left ventricular cross-sectional surface. For renal sections, each immune cell type was quantified separately using a semiquantitative scale as follows: grade 0, no leukocytes present; grade 1, single leukocytes in the field of view; grade 2, single leukocyte aggregates per section; and grade 3, many leukocyte aggregates per section. The mean calculated from independently assessed values of the different leukocytes is presented as an inflammation cell index.

The left ventricle apoptosis Terminal deoxynucleotidyl transferase dUTP nick end labeling (TUNEL) staining of cardiac sections was performed using an CardioTACS In Situ Apoptosis Detection kit (Trevigen) according to the manufacturer's protocol. DNA fragmentation was visualized by the incorporation of biotinylated nucleotides, binding streptavidin-horseradish peroxidase and followed by reaction with TACS Blue Label™, which generated a dark-blue precipitate. Tissue sections were counterstained with Nuclear Fast Red to visualize TUNEL-negative nuclei. For each longitudinal left ventricular section, the number of TUNEL + nuclei was scored and presented as the mean numerical density per $0.1 \, mm^2$ of the left ventricular cross-sectional surface.

Data analysis All results are expressed as the mean ± S.E. M. Concentration–response curves (CRCs) were constructed based on the responses to cumulative concentrations of the studied compounds and analyzed by nonlinear curve fitting using GraphPad Prism 5.0 (GraphPad Software, Inc., San Diego, CA, USA). Relaxations are expressed as a percentage of inhibition of the maximal tension obtained with the contractile agent (Emax = 100%).

Statistically significant differences between groups were calculated using either one-way or two-way analysis of variance (ANOVA) and the post hoc Bonferroni or Dunn multiple comparison test. Two-way ANOVA was applied for the "measurement of systolic blood pressure" experiment to determine how a response is affected by two factors. One-way ANOVA was applied for the rest of the experiments. The criterion for significance was set at $P < 0.05$.

Results

Effect of MH-76, MH-79, and prazosin on systolic blood pressure and heart rate

A significant increase in systolic blood pressure during DOCA-salt treatment was observed in all DOCA-salt treated rats compared to that in the control group at the end of 6 weeks. Treatment with MH-76, MH-79 (10 mg/kg), and prazosin (0.4 mg/kg) had antihypertensive effects and prevented further increases in SBP during the last 6 weeks (Fig. 1a). Prazosin reduced the systolic blood pressure to near control values in the 1st week of administration, and its effect persisted until the end of the experiment. The tested compounds MH-76 and MH-79 also lowered the blood pressure; however, they exhibited a 1-week latency period. Comparing the antihypertensive potency, prazosin was superior to MH-76, and MH-79 caused a faster and greater drop in systolic blood pressure (Fig. 1a). However, at the end of the experiment, the values of systolic blood pressure in rats treated with DOCA-MH-76, MH-79, or prazosin did not differ significantly (Fig. 1b).

DOCA-salt rats showed a higher heart rate in comparison to normal control rats. Treatment with MH-79 but not with prazosin diminished the higher heart rate ((Fig. 1c).

Effect of MH-76, MH-79, and prazosin on body and organ weight and biochemical parameters

There were no significant differences in body weight in all groups; however, DOCA-salt rats showed the lowest body weight (Fig. 2a). DOCA-salt rats showed heart hypertrophy as evidenced by heart wet weight relative to body weight (Fig. 2c). Treatment of DOCA-salt rats with MH-76 and MH-79 significantly reduced the increased heart weight compared to DOCA-salt rats with no treatment. In contrast, the increased heart weight was not affected by prazosin treatment.

The morphometric analysis showed a significant increase in left ventricular wall thickness in DOCA-salt rats compared to that in the control animals (Fig. 2d). The studied compounds abolished the increase, with prazosin being the most and MH-76 being the least effective, which corresponds well to their hypotensive activity.

The kidney/body weight ratio was also increased in DOCA-salt rats. Treatment with MH-76 and MH-79 reduced kidney hypertrophy; however, the effect of prazosin on kidney weight was not significant (Fig. 2b).

The concentration of plasma norepinephrine in DOCA-salt hypertensive rats was lower than that in normal controls, probably as a compensatory effect of elevated blood pressure. Treatment with MH-76 and MH-79 showed an antihypertensive effect, but there was no increase in the norepinephrine concentration. However, treatment with prazosin caused an increase in the norepinephrine concentration compared to that in DOCA-salt rats (Table 1).

There were no significant differences in serum creatinine and urea levels among the control and treatment groups (Table 1).

Effect of MH-76, MH-79, and prazosin on proinflammatory markers, lipid peroxidation, and NPSH levels

The serum level of CRP was significantly higher in DOCA-salt hypertensive rats. Chronic α1-blockade with MH-76, MH-79, and prazosin markedly decreased CRP levels in comparison to those in DOCA-salt and normal control rats (Fig. 3a).

The level of IL-6 in kidney homogenates was significantly higher in DOCA-salt hypertensive rats, as well as in DOCA-salt rats treated with MH-79. Treatment with
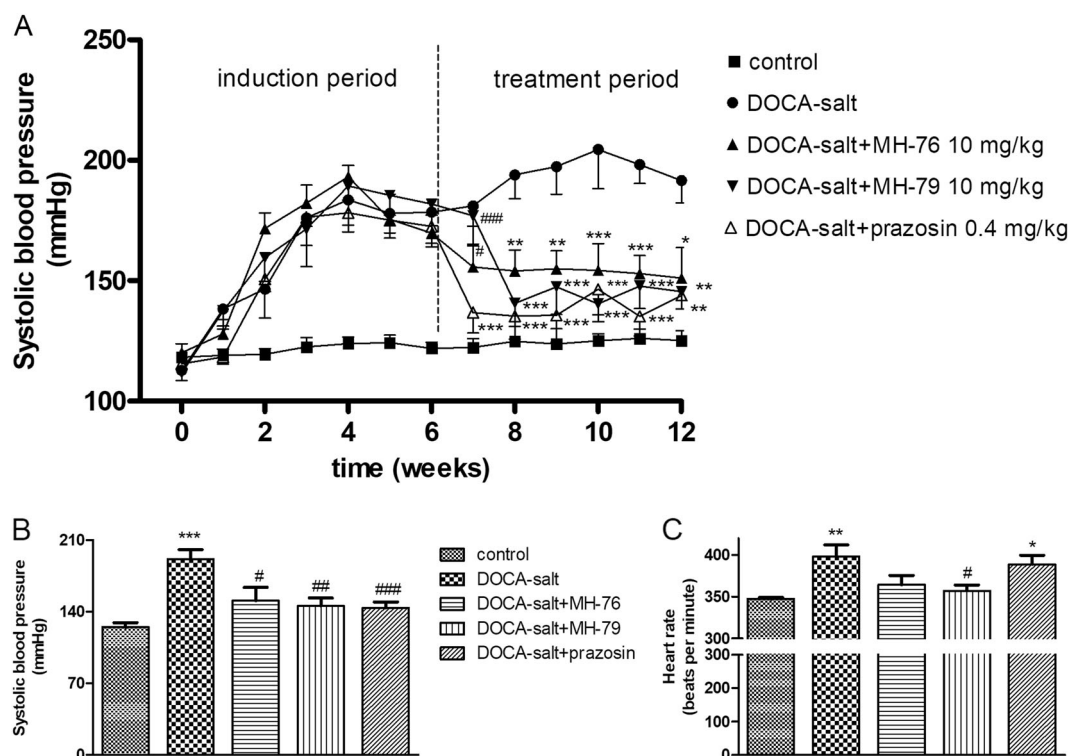
Fig. 1 **a** Effects of MH-76, MH-79 (10 mg/kg i.p.), and prazosin (0.4 mg/kg i.p.) on systolic blood pressure in DOCA-salt hypertensive rats. Values are expressed as means ± SEM (n = 6-8), #P < 0.05, ##P < 0.01 vs. control; *P < 0.05, **P < 0.01, ***P < 0.001 vs. DOCA-salt (two-way ANOVA, post hoc Bonferroni test), **b** Systolic blood pressure, and **c** heart rate of control, DOCA-salt, DOCA-salt + MH-76–treated, DOCA-salt + MH-79–treated, and DOCA-salt + prazosin-treated rats at the end of the experimental period. Values are expressed as means ± SEM (n = 6–8), *P < 0.05, **P < 0.01, ***P < 0.001 vs. control; #P < 0.05, ##P < 0.01, ###P < 0.001 vs. DOCA-salt, (one-way ANOVA, post hoc Bonferroni test)

MH-76 normalized the kidney IL-6 concentration, whereas prazosin markedly increased the IL-6 level even in comparison to that in DOCA-salt rats (Fig. 3b).

The level of MDA in kidney homogenates was significantly higher in DOCA-salt hypertensive rats (Fig. 3c). Treatment with MH-76 but not with prazosin decreased the concentration of the markers of lipid peroxidation. The level of NPSH in kidney homogenates was significantly lower in DOCA-salt hypertensive rats than in normal controls (Fig. 3d). Treatment with MH-76, MH-79, and prazosin increased the concentration of nonprotein thiols.

Effect of MH-76, MH-79, and prazosin on endothelial dysfunction

Thoracic aortic rings from DOCA-salt hypertensive rats showed decreased relaxation responses to carbachol, suggesting vascular endothelial dysfunction (Fig. 4). The maximum relaxation of vessels in the DOCA-salt hypertensive rat group amounted to ~70%. Treatment with the studied compounds, especially MH-79, normalized this altered endothelial response. The CRC for DOCA-salt, DOCA-salt + MH-76, and DOCA-salt + prazosin were shifted to the right relative to the control group. Treatment

with MH-79 was the most effective regarding endothelial dysfunction—there was no displacement of the CRC to the right, and aortas from the DOCA-salt + MH-79 group showed a degree of relaxation comparable with that of the normal control (Fig. 4).

Effect of MH-76, MH-79, and prazosin on heart and kidney histopathology

Effect of MH-76, MH-79, and prazosin on cardiac arteriosclerosis and hyalinosis

The cardiac arteriosclerotic index presented here is a cumulative indicator of signs of arteriosclerotic histopathological alteration in arterial walls and the perivascular area of arteries of left ventricles and involves foam cell abundance, perivascular fibrosis severity, and immune/inflammatory cell accumulation in the perivascular area (Fig. 5a, Masson's trichrome staining). By contrast, the coronary atherosclerotic plaque formation index for small arteries and arterioles focused on changes closest to the tunica intima and was scored as the summation of macrophage infiltration, foam cells occurrence, intracellular and extracellular lipid formation, smooth muscle cell migration, epithelial cell
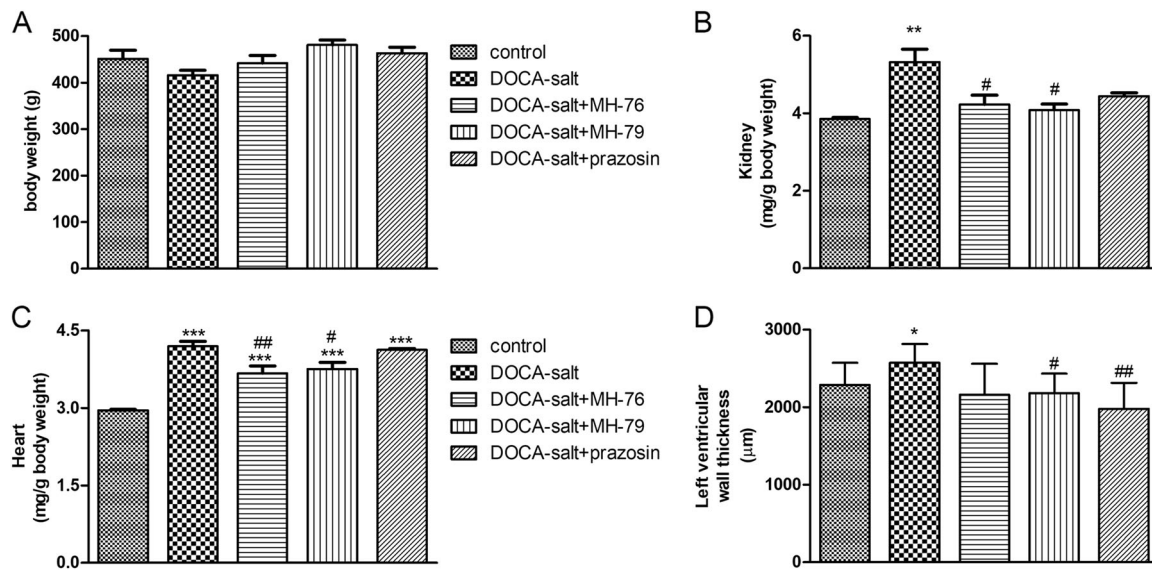
Fig. 2 Body weight (**a**), kidney weight (**b**), heart weight (**c**), and left ventricular wall thickness (**d**) of control, DOCA-salt, DOCA-salt + MH-76–treated, DOCA-salt + MH-79–treated and DOCA-salt + prazosin-treated rats at the end of the experimental period. Values are expressed as means ± SEM ($n = 6$–8), $*P < 0.05$, $**P < 0.01$, $***P < 0.001$ vs. control; $\#P < 0.05$, $\#\#P < 0.01$ vs. DOCA-salt, (one-way ANOVA, post hoc Bonferroni test)

Table 1 Norepinephrine, creatinine and urea serum concentration of control, DOCA-salt–treated, DOCA-salt + MH-76–treated, DOCA-salt + MH-79–treated, and DOCA-salt + prazosin-treated rats at the end of the experimental period

Parameter	Control	DOCA-salt	DOCA-salt+MH-76	DOCA-salt+MH-79	DOCA-salt+prazosin
Biochemical parameters					
Norepinephrine (ng/ml)	10.3 ± 0.4	7.5 ± 0.7*	8.3 ± 0.6	8.9 ± 0.6	10.0 ± 0.6**
Creatinine (nmol/ml)	104.1 ± 11.4	100.1 ± 10.4	104. ± 11.8	102.2 ± 6.4	86.1 ± 14.3
Urea (ng/ml)	124.8 ± 6.0	134.5 ± 7.5	119.2 ± 7.7	128.0 ± 10.6	139.5 ± 7.4

$n = 7$–8

DOCA deoxycorticosterone acetate

$*P < 0.05$ vs control, $**P < 0.05$ vs DOCA-salt

transformation, and damage to the tunica intima. The coronary atherosclerotic plaque formation index is shown in Fig. 6e for better comparison with similar processes within renal arteries (Fig. 6a, c, d). A significant increase in the severity of specified processes was observed following DOCA-salt treatment compared with that in the control group. Treatment with MH-79 was the most effective in reversing the DOCA-salt arteriosclerotic and atherosclerotic effects (Figs. 5c, 6b, e). Hyaline arteriopathy of the smallest cardiac arterioles was evident in the DOCA-salt group, and all studied compounds showed a tendency to reverse this hyalinotic effect (Fig. 5a, PAS staining). We also investigated the calcification of the wall of coronary arteries from the left ventricle. Statistically significant calcified lesions were observed only in the coronary arterial intima in the DOCA-salt + prazosin group (0.85 ± 0.45 vs 0.0 ± 0.0 for the control group, DOCA-salt, DOCA-salt + MH-76, DOCA-salt + MH-79, $P < 0.05$) (Fig. 7). Calcification of

coronary arteries was not observed in the DOCA-salt- and DOCA-salt + MH-76 and +MH-79 groups. DOCA-salt treatment did not cause calcification in the coronary arteries. Calcified areas were detectable by Von Kossa staining.

Effect of MH-76, MH-79, and prazosin on renal atherosclerotic injury and vessel remodeling

The intrarenal principal branches of the kidney artery were microscopically semiquantitatively assessed for different parameters of atherosclerotic injury (Fig. 6a). The involved processes (e.g., leukocyte (monocyte) accumulation and adhesion to endothelium, endothelial damage and dysfunction, inflammatory cell accumulation within the tunica intima, occurrence of foam cells, fatty streak and fibrous cap formation, and internal elastic lamina fenestration) were significantly higher in the DOCA-salt group than in the control group and were beneficially reduced by the
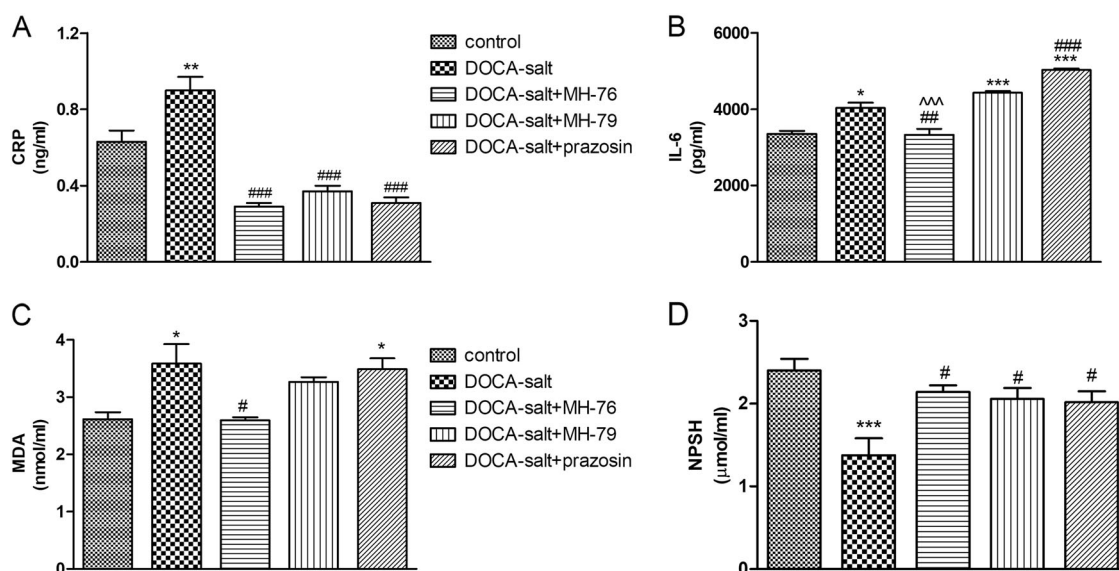
Fig. 3 a Serum CRP, b kidney IL-6, c kidney MDA, and d kidney NPSH concentration of control, DOCA-salt, DOCA-salt + MH-76–treated, DOCA-salt + MH-79–treated, and DOCA-salt + prazosin-treated rats at the end of the experimental period. Values are expressed as means ± SEM ($n = 6$–8), $*P < 0.05$, $**P < 0.01$, $***P < 0.001$ vs. control; $\#P < 0.05$, $\#\#P < 0.01$, $\#\#\#P < 0.001$ vs. DOCA-salt, $\wedge\wedge\wedge P < 0.001$ vs. DOCA-salt + prazosin-treated rats (one-way ANOVA, post hoc Bonferroni test)

Fig. 4 a Cumulative concentration–response curves for carbachol and b maximal relaxation in thoracic aortic rings from control, DOCA-salt–treated, DOCA-salt + MH-76–treated, DOCA-salt + MH-79–treated and DOCA-salt + prazosin-treated rats. Values are expressed as means ± SEM ($n = 6$–8), $*P < 0.05$, $***P < 0.001$ vs. control; $\#\#P < 0.01$, $\#\#\#P < 0.001$ vs. DOCA-salt, (one-way ANOVA, post hoc Bonferroni test)
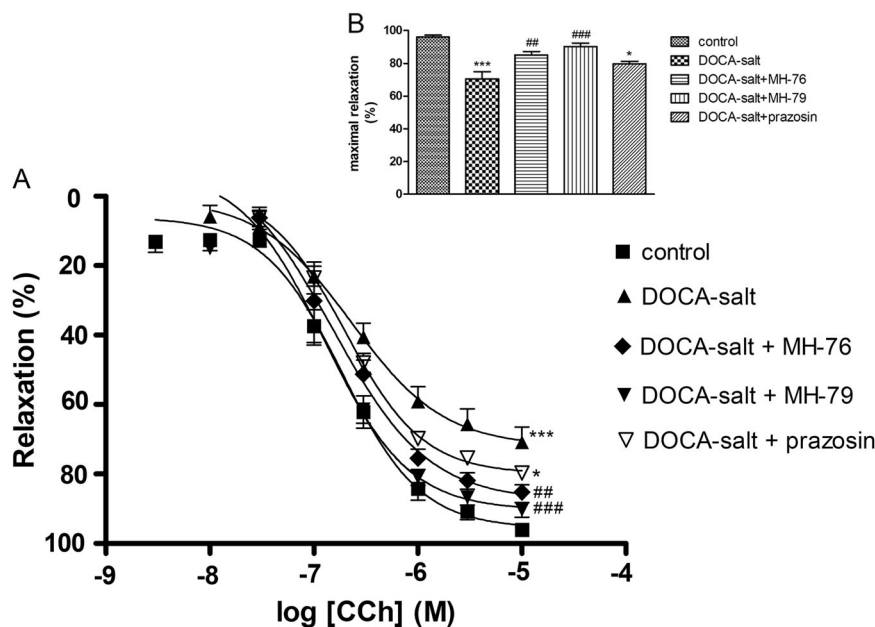

treatments with all examined compounds; however, treatment with prazosin was the least effective (Fig. 6a, c). Independent of the phenomena listed above occurring mainly in the tunica intima, the fibroplastic remodeling of the tunica media of renal arteries of DOCA-salt-treated animals was markedly increased compared to that of control rats (Fig. 6d). The effect was even strengthened by prazosin treatment compared to the effect in the DOCA-salt group and was accompanied by disorder of the shape and orientation of the smooth muscle cells (seen by PAS staining); in

addition, phenotypic alteration of smooth muscle cells was unmasked by varied staining with Masson's trichrome (Fig. 6a).

Effect of MH-76, MH-79, and prazosin on cardiac left ventricular and renal sclerotic injury

The morphometric analysis of myocardial interstitial fibrosis after picrosirius red staining showed a significant increase in all DOCA-salt treated animals compared with

A

| Picrosirius Red | PAS | Masson`s Trichrome |

B

C
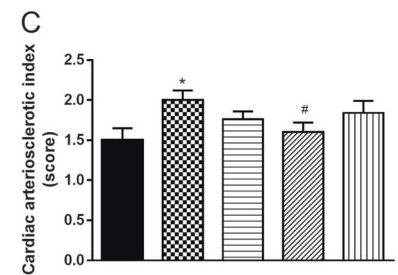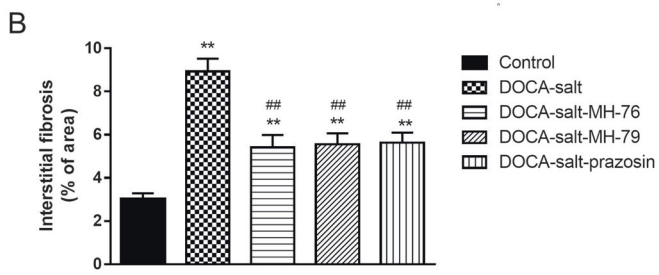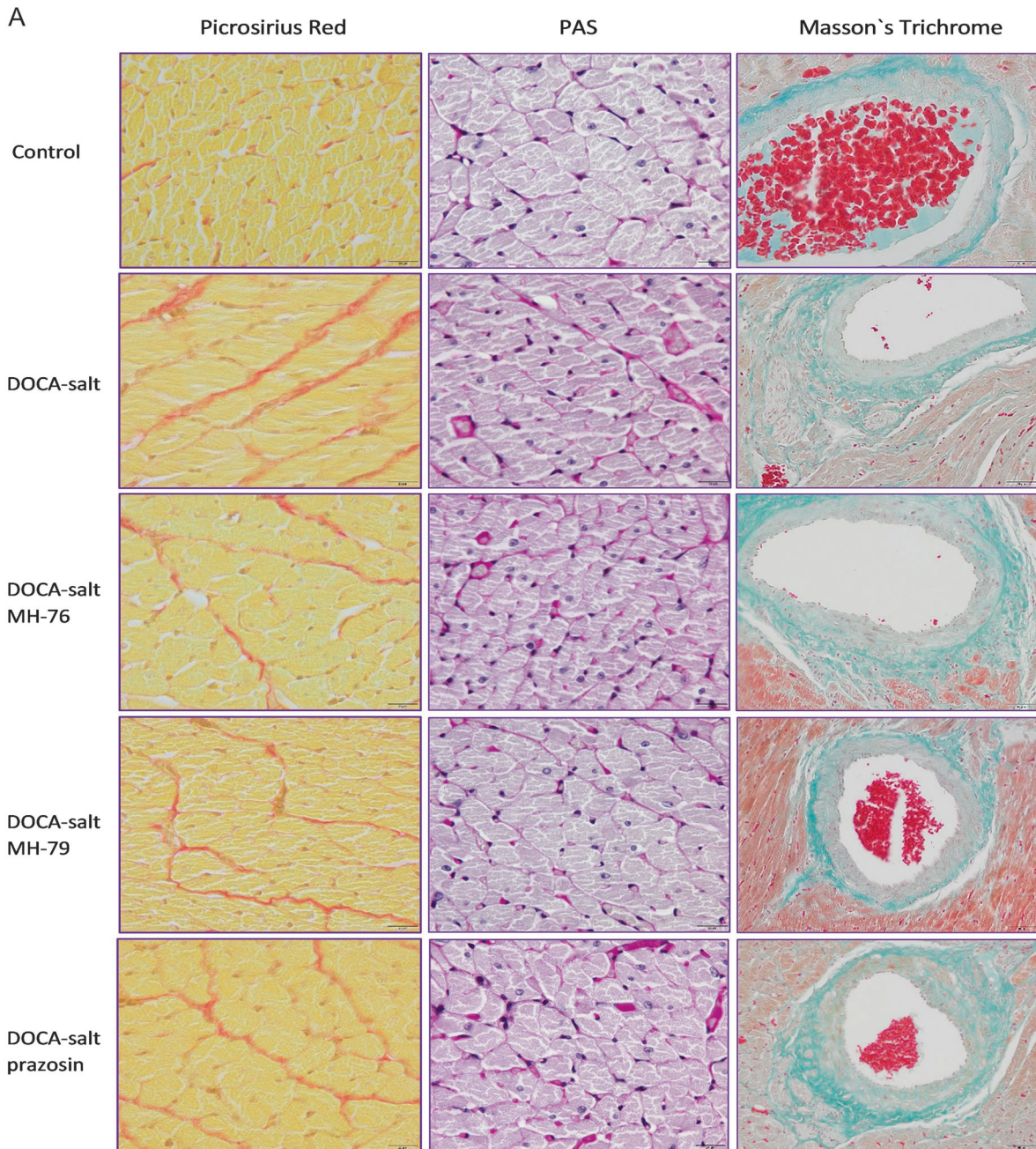
Fig. 5 a Representative pictures of perivascular and interstitial fibrosis (picrosirius red staining (bar 20 μm)), hyalinosis (PAS staining), arteriosclerosis (Masson's trichrome staining) in the left ventricle of control, DOCA-salt–treated, DOCA-salt + MH-76–treated, DOCA-salt + MH-79–treated and DOCA-salt + prazosin-treated rats. **b** Quantification of myocardial interstitial fibrosis and **c** the cardiac arteriosclerotic index in the different groups of rats. The data are expressed as means ± S.E.M. *$P < 0.05$, **$P < 0.01$ vs. control group and #$P < 0.05$, ##$P < 0.01$ compared with the DOCA-salt hypertensive group

that in the control group (Fig. 5a). However, MH-76, MH-79, and prazosin treatments significantly reduced the myocardial fibrosis caused by DOCA-salt administration (Fig. 5b). Representative pictures of PAS-stained left ventricular sections of all examined groups (Fig. 5a) showed that the hyalinotic effect in the left ventricle was comparable to that presented by fibrosis.

In the kidney, morphologic examination determined by picrosirius red and PAS staining showed tubular dilatation with cast formation, thickening of the tubular membrane, fibrosis and focal tubular atrophy mainly in DOCA-salt-treated, DOCA-salt + MH-76-treated, and DOCA-salt + prazosin-treated rats (Fig. 8a). The tubulointerstitial sclerotic index was ~5-fold greater in DOCA-salt-treated rats than in control rats. Furthermore, treatment with all studied compounds significantly reduced tubulointerstitial injury, with MH-79 being the most effective (Fig. 8b).

Picrosirius red and PAS staining revealed collagen deposition in glomerular Bowman's capsule in DOCA-salt hypertensive rats. In all groups of rats receiving DOCA-salt, we also observed focal segmental glomerulosclerosis, compressed capillary loops, mesangial nodular deposits, and crescents obliterating the glomerular space (Fig. 8a). The glomerular sclerotic index was markedly higher in all DOCA-salt-receiving rats than in control animals, and only prazosin treatment significantly reduced the glomerular sclerotic index (Fig. 8c).

Effect of MH-76, MH-79, and prazosin on cardiac left ventricular and renal infiltration by leukocytes

In the heart, only mast cells were found. The cells principally showed an interstitial location, and only a few were found in the pericardium. The mean numerical density of mast cells was significantly higher in all DOCA-salt-treated groups compared with the control group (Supplementary Figure 2C). High magnification of mast cells infiltrating the interstitial area of the left ventricle is shown in Supplementary Figure 2A, B.

In the kidney, the cumulative index of infiltration of various inflammatory immune cells (neutrophils, macrophages, mast cells, and lymphocytes) was significantly higher in the DOCA-salt-treated, DOCA-salt + MH-76-treated, and DOCA-salt + prazosin-treated groups than in

the control group (Fig. 9b). Only treatment with MH-79 significantly reduced the leukocyte infiltration caused by DOCA-salt administration. Representative high-power pictures of glomerular neutrophils, tubulointerstitial macrophages, infiltration of mast cells in the wall of the minor calyx and infiltration of lymphocytes in the renal cortex are shown in Fig. 9a.

Effect of MH-76, MH-79, and prazosin on cardiac left ventricular apoptosis

To identify apoptotic nuclei in tissue sections, we used the CardioTACS In Situ Apoptosis Detection kit. TUNEL-positive cells exhibited dark-blue stained nuclei. In the cardiac left ventricle, the numerical density of TUNEL-positive nuclei did not show significant changes among the examined groups, even if a slight increase in TUNEL-positive nuclei in DOCA-salt-treated and DOCA-salt + prazosin-treated rats was observed (Supplementary Figure 3).

Discussion

The DOCA-salt hypertensive rat is an established model of malignant mineralocorticoid hypertension with renal dysfunction [14]. The administration of DOCA, in combination with salt loading in the diet, induces increased renal sodium reabsorption, resulting in hypervolemia [2, 15]. These conditions lead to symphatoexcitation and a rise in blood pressure due to increased vessel smooth muscle tone and peripheral vascular resistance. The hypertension induced by these factors later leads to endothelial dysfunction, cardiovascular remodeling, left ventricle hypertrophy, fibrosis, and heart failure [2, 15]. Alongside cardiovascular remodeling, kidney damage with glomerulosclerosis and tubular fibrosis appears. There is evidence that in the pathomechanism of DOCA-salt-evoked volume-dependent hypertension and end organ damage, increased oxidative stress and inflammation are highly involved. Accordingly, this model emphasizes the role of the sympathetic nervous system, reactive oxygen species (ROS) and inflammation in the development of renal and cardiovascular remodeling [2, 14, 15].

In the present study, we investigated the effect of **MH-76** and **MH-79** on DOCA-salt hypertension in rats; these two compounds have α1-adrenoceptor blocking properties and an ability to stimulate the NO/cGMP/K + channel pathway [12, 13]. The compounds were administered to animals with established severe hypertension, and their therapeutic effect was evaluated. We aimed to compare the classic α1-adrenoceptor blocker prazosin with multifunctional, new agents in the DOCA-salt model of malignant hypertension.
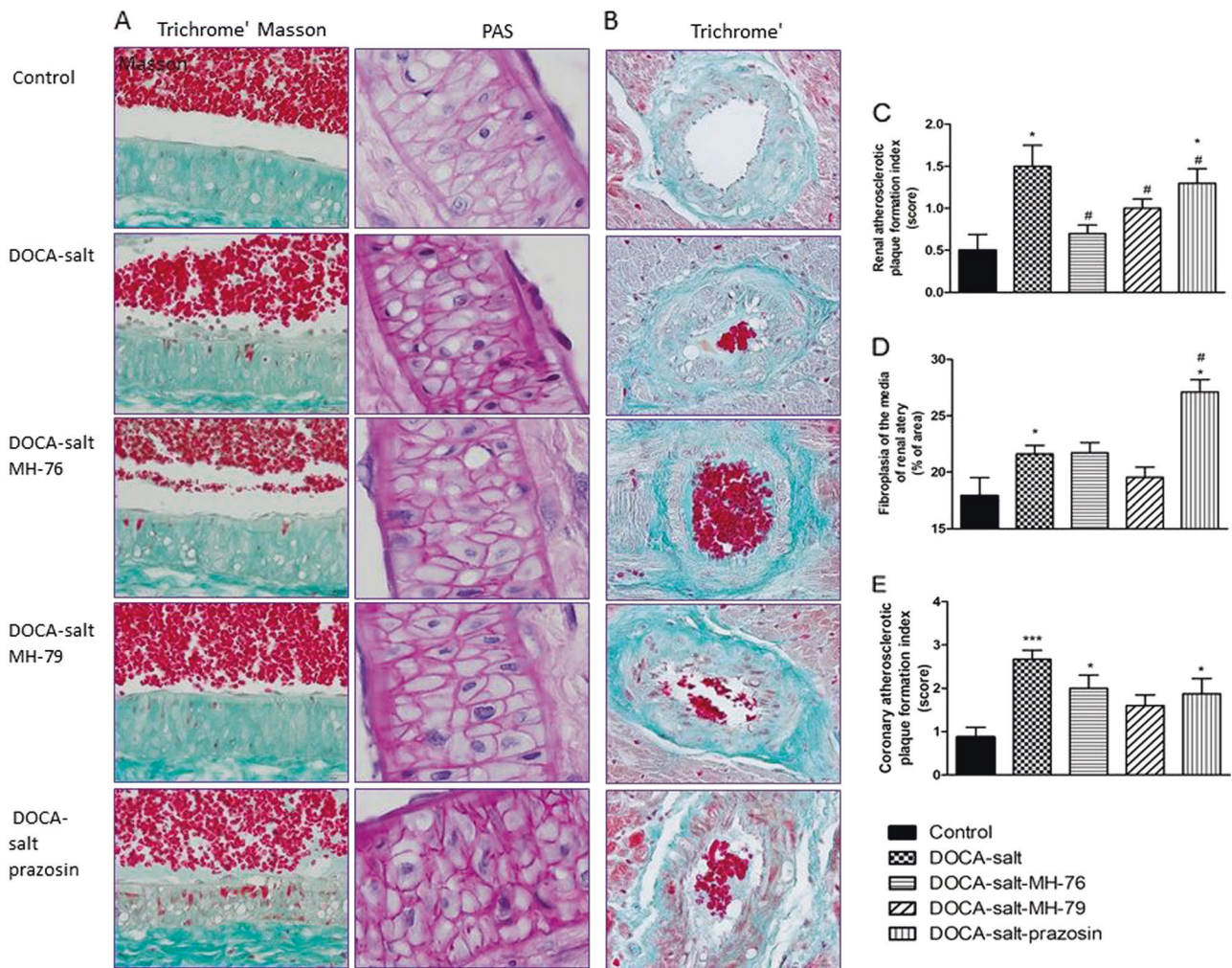
Fig. 6 Representative histological pictures of control, DOCA-salt–treated, DOCA-salt + MH-76–treated, DOCA-salt + MH-79–treated and DOCA-salt + prazosin-treated rats: **a** Renal atherosclerotic plaque formation and fibroplasia of the tunica media of the wall of the intrarenal segmental branch of the artery (longitudinal cross-sections). Left column, atherosclerotic plaque formation (Masson's trichrome, bar: 50 μm). Right column, subadventitial-perimuscular fibroplasia of the tunica media (PAS, bar: 20 μm). **b** Coronary atherosclerotic plaque formation. Masson's trichrome, bar: 20 μm (transversal cross-sections). **c** Severity of renal atherosclerotic plaque formation in the different groups of rats. **d** Quantification of fibroplasia of the tunica media of the intrarenal segmental branch of the artery. **e** Severity of coronary atherosclerotic plaque formation in the different groups of rats. The data are expressed as means ± S.E.M. $*P < 0.05$, $***P < 0.001$ compared with the control group and $\#P < 0.05$ compared with the DOCA-salt hypertensive group

We chose prazosin as the reference compound for a few reasons. First, prazosin and the studied compounds share the main mechanism of action (α1-adrenoceptor blockade). Second, prazosin, as a quinazoline derivative, may exert proapoptotic and necrotic effects, whereas the studied compounds do not contain a quinazoline moiety and are devoid of cardiotoxic effects (unpublished data). Next, quinazoline-based α1-adrenolytics (prazosin, doxazosin) have been mainly used in the pharmacotherapy of cardiovascular diseases; however, the presence of a quinazoline moiety may have limited the beneficial effects resulting from α1-adrenoceptor blockade. It is worth mentioning that prazosin and the studied compounds were administered at equivalent doses with respect to their affinity for α1-adrenoceptors. The doses of **MH-76** and **MH-79** were higher than the dose of prazosin due to the difference in their affinities for α1-adrenoceptors (Ki prazosin = 0.1 nM, Ki MH-76, MH-79 = ~2 nM) [11].

This study showed that administration of **MH-79** and, to a lesser extent, **MH-76** decreased elevated systolic blood pressure and heart rate, reduced heart and kidney hypertrophy and reversed the histopathological alterations of heart and kidney and vessels in DOCA-salt hypertensive rats. Furthermore, the test compounds, especially **MH-79**, revealed a protective effect on the endothelium and the ability to reverse endothelial dysfunction. Prazosin showed a potent hemodynamic effect and reduced cardiac and renal fibrosis but exerted an unfavorable effect on blood vessels,

Fig. 7 Representative
photomicrographs of von Kossa
staining in the left ventricle
demonstrating calcification
within the wall of coronary
blood vessels. Arrows indicate
sites of calcification
(mineralization). Bar: 100 μm
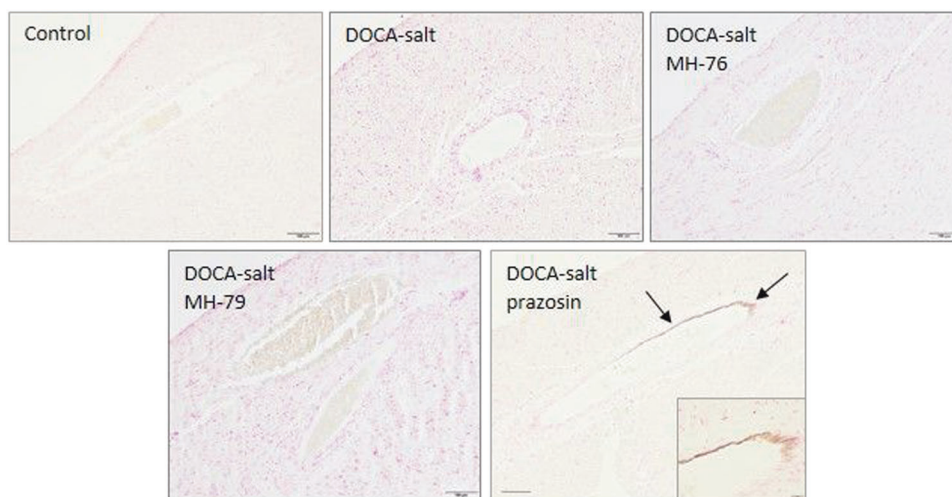
potentiating fibroplasia of the media of the intrarenal artery and causing calcification of coronary arteries. In contrast to the studied compounds, prazosin did not reduce endothelial dysfunction.

First, it must be emphasized that the studied compounds showed significant antihypertensive activity and effectively reduced elevated blood pressure after a 1-week latency period, but their effect persisted until the end of the experiment, and resistance was not observed. Prazosin decreased arterial pressure in the first week of administration and showed the strongest hypotensive effect.

There are many antihypertensive drugs that have no effect on blood pressure in the DOCA-salt model of malignant hypertension, or after their initial effectiveness, resistance appears [19, 20]. The studied compounds as well as prazosin effectively reduced elevated blood pressure. However, although the hypotensive activity of the studied compounds was weaker than that of prazosin, their final effect was more beneficial.

In histopathological studies, we found that all studied α1-adrenolytics decreased cardiac interstitial fibrosis and left ventricle wall thickening. Moreover, the studied compounds, but not prazosin, reduced cardiac hypertrophy, as evidenced by heart/body weight indexes.

The process of pathological cardiovascular remodeling, cardiac fibrosis and hypertrophy is complex and includes hemodynamic overload and biochemical pathways associated with oxidative stress and inflammation [15]. However, hemodynamic factors with sympathetic nerve overactivity are potent regulators in the pathogenesis of left ventricular hypertrophy and fibrosis [14, 21]. Sympathetic overdrive produces peripheral vasoconstriction, activates other neurohumoral systems (renin-angiotensin, vasopressin, endothelin), increases myocardial oxygen consumption and exerts direct proapoptotic and pronecrotic effects [21]. Studies performed by Perlini [21] demonstrated

that α-blockade depressed cardiac fibrosis in the rat model of hypertensive heart disease. Consistently, the beneficial effect on cardiac fibrosis and left ventricle wall thickening of all tested compounds may be attributed to their blood pressure lowering effect and α1-adrenoceptor blockade. However, prazosin was less effective in reducing heart weight and did not reduce the heart rate. On the other hand, the hypotensive effect of **MH-76** and **MH-79** was not accompanied by reflex tachycardia; by contrast, treatment with the studied compounds, especially **MH-79**, decreased the heart rate. The studied compounds, 1-(2-methoxyphenyl)piperazine derivatives, may be regarded as urapidil analogs, and similarly to urapidil, they are also 5-HT1A serotoninergic receptor ligands [22]. It is possible that the compounds reduce the sympathetic drive by acting on central 5-HT1A receptors, which prevents reflex tachycardia [23–25].

In addition, we observed an increased norepinephrine concentration following prazosin treatment. We claim that prazosin did not prevent adrenergic stimulation as effectively as the tested compounds did, which was manifested in the higher plasma norepinephrine concentration and higher heart rate of DOCA-salt prazosin-treated rats. We think that prazosin-evoked adrenergic activation may explain why prazosin did not effectively reduce heart hypertrophy.

DOCA-salt rats are also a model for studying kidney damage in the setting of hypertension. DOCA-salt rats developed renal injury with tubulointerstitial fibrosis, glomerulosclerosis, and renal hypertrophy due to mineralocorticoid insult with subsequent volume overload [20, 26]. The inflammation, increased expression of proinflammatory cytokines and ROS generation were also shown to be involved in the initiation and progression of glomerulosclerosis and tubulointerstitial fibrosis [27], and we detected inflammatory cells in the kidneys of DOCA-salt
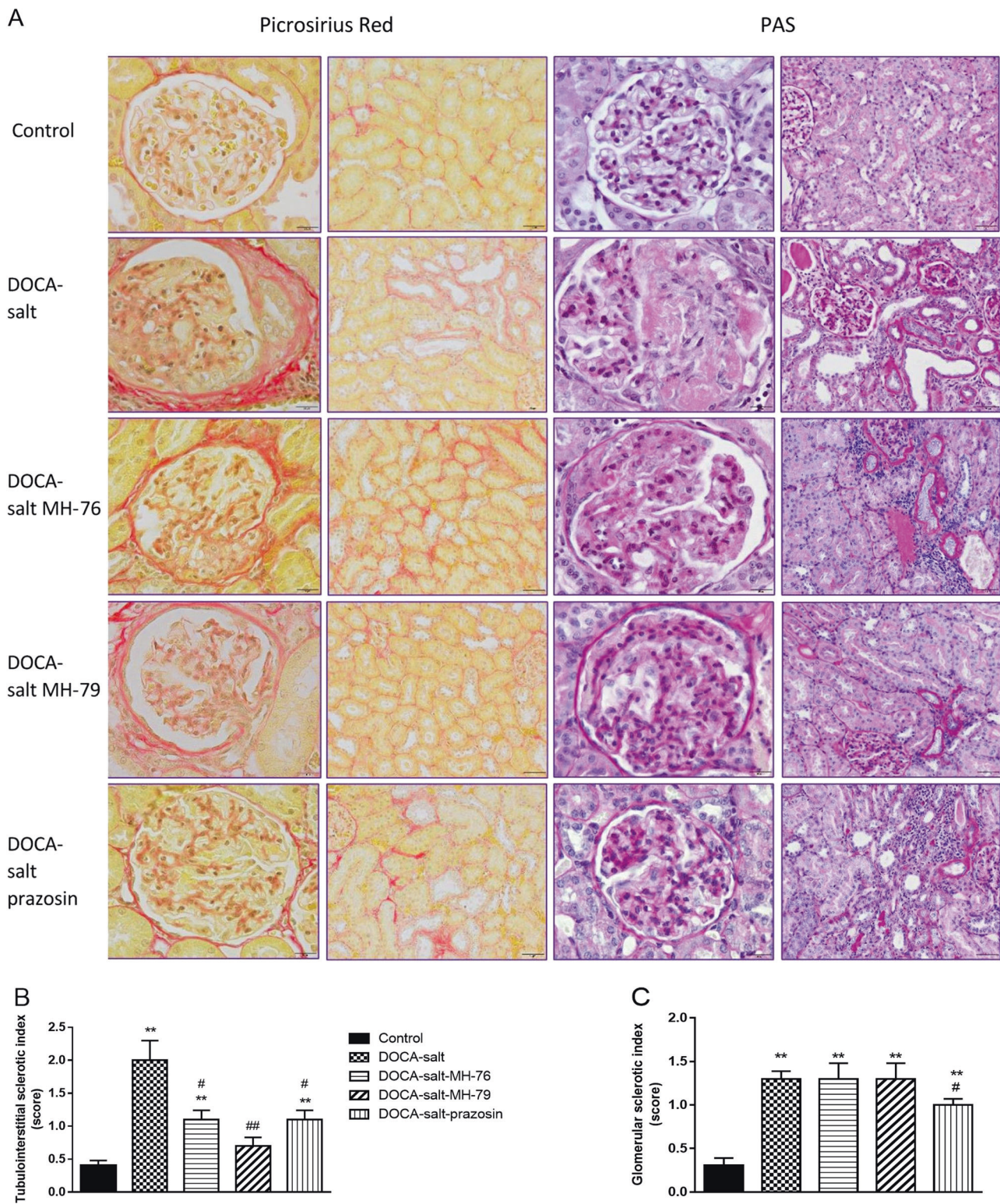
Fig. 8 a Representative histological pictures of the glomerular (bar: 20 μm) and tubulointerstitial (bar: 50 μm) sclerosis of the control, DOCA-salt, and DOCA-salt hypertensive rats treated with MH-76, MH-79, and prazosin. Picrosirius red staining reveals collagen deposition in glomerular Bowman's capsule in DOCA-salt hypertensive rats. PAS staining images show tubule dilation, atrophy, cast formation and thickening of the tubular membrane in the DOCA-salt hypertensive group. Index of tubulointerstitial (**b**) and glomerular (**c**) sclerosis in the different groups of rats. Sclerosis was scored on a scale from 0 to 5 as described in the Materials and Methods section. The data are expressed as means ± S.E.M. $**P < 0.01$ compared with the control group and $\#P < 0.05$, $\#\#P < 0.01$ compared with the DOCA-salt hypertensive group

Fig. 9 a Representative histological pictures of kidney sections with infiltration of leukocytes. Glomerular neutrophils and tubulointerstitial macrophages (PAS staining, bar: 20 μm), infiltration of lymphocytes in the renal cortex (PAS staining, bar: 100 μm) and infiltration of mast cells in the wall of the minor calyx (May–Grunwald staining, bar 100 μm). b Index of infiltration of leukocytes in the different groups of rats. Data are expressed as means ± S.E.M. *P < 0.05, ***P < 0.001 compared with the control group and #P < 0.05 compared with the DOCA-salt hypertensive group
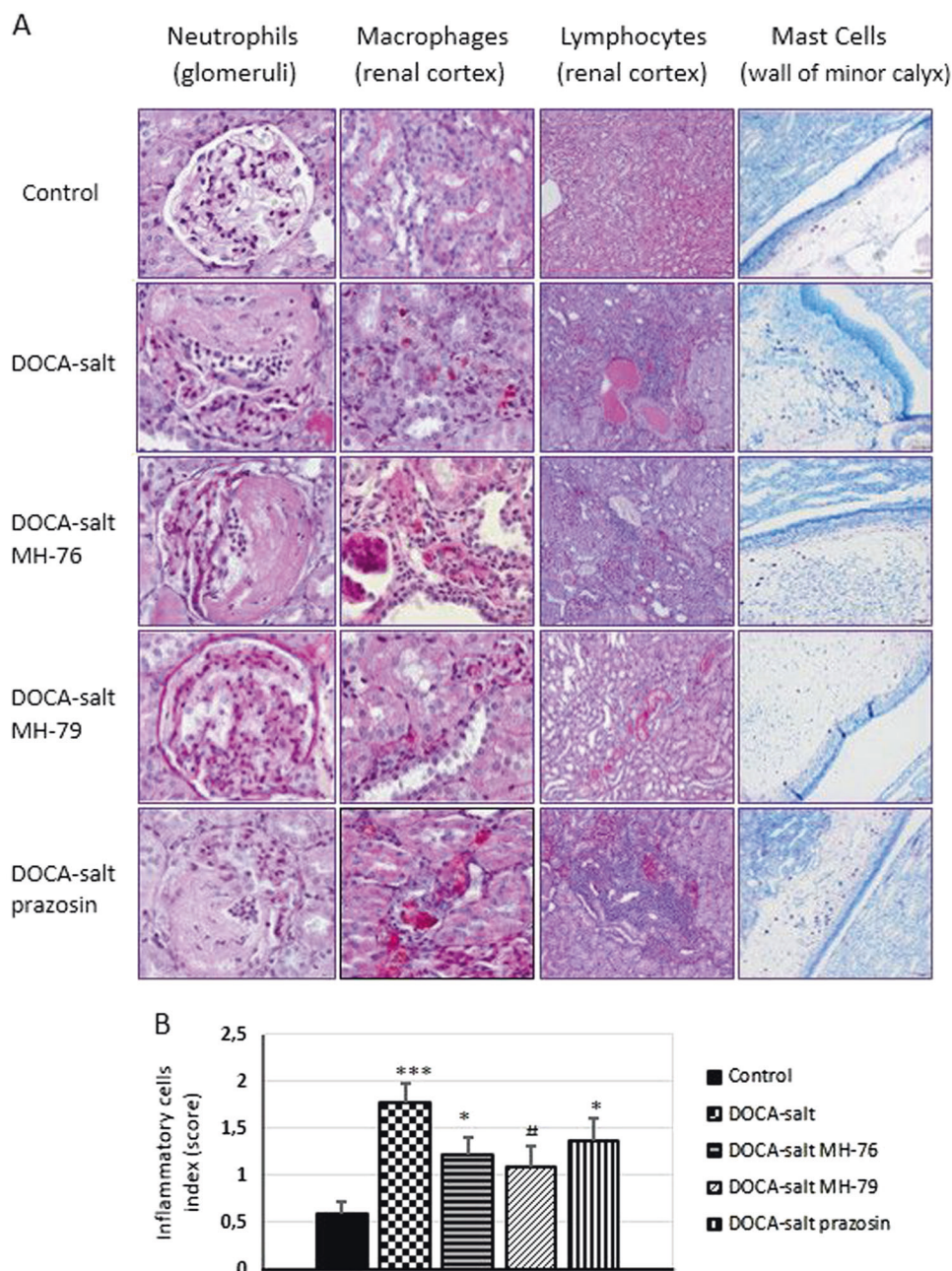
rats. Glomerular injury was alleviated by prazosin treatment only, and we claim that this effect was strongly attributed to its most potent hypotensive activity. However, there are studies reporting that α1B-adrenoceptor blockade exerts an antifibrotic effect in human mesangial cells due to modulation of the kallikein–kinin system, independently of the hemodynamic effects [28]. This effect may also account for the beneficial influence of prazosin on glomerulosclerosis because prazosin is a nonselective α1-adrenoceptor antagonist, whereas the studied compounds are α1A/α1D-adrenoceptor antagonists [12]. On the other hand, tubulointerstitial damage was reduced by all examined α1-adrenolytics, with **MH-79** being the most effective. Moreover, the number of inflammatory cells within the kidney was closely associated with the severity of tubulointestital lesions, **MH-79** was the only compound able to reduce inflammatory cell infiltration, and **MH-79** was the most potent in reducing tubulointerstitial fibrosis. Tubulointerstitial injury may be the result of hypertension, endothelial damage, oxidative stress, and inflammation with leukocyte infiltration, which are all well documented in the DOCA-salt model [20, 27].

The endothelium plays diverse roles in the cardiovascular system, including vasomotor, antioxidant, and anti-

inflammatory activities. Endothelial cells form a functional and structural barrier between the blood and the vascular wall. Intercellular junctions between endothelial cells mediate barrier function. The healthy endothelium has anti-inflammatory properties, whereas proinflammatory stimuli damage the junctions, leading to the impairment of the endothelial barrier and increased junctional permeability. This promotes transendothelial migration of inflammatory cells to the arterial intima. As a consequence of the influx of immune cells, an induction of vascular inflammation and fibrosis appears [29–31]. Endothelial dysfunction contributes markedly to the pathogenesis and progression of hypertension [32], and among other mechanisms, hypertension contributes significantly to endothelial dysfunction due to elevation in shear stress and the promotion of chronic low-grade inflammation. Circulating proinflammatory cytokines cause ROS production in the endothelium, which induces oxidative NO inactivation as superoxide anions react with NO and form peroxynitrite [26, 30, 31].

The main feature of endothelial dysfunction is the loss of the protective actions of NO due to reduced synthesis from endothelial NO synthase and/or increased scavenging by ROS. Decreased NO bioavailability upregulates the endothelial expression of adhesion molecules, which induces inflammatory cell infiltration and promotes smooth muscle cell activation, proliferation, and migration [30, 31]. We observed endothelial dysfunction through decreased responses to carbachol, an analog of acetylcholine, in isolated aortas of DOCA-salt hypertensive rats. We previously reported that in contrast with prazosin, **MH-79** and **MH-76** were able to activate endothelial NO generation and endothelium-dependent cGMP production [13]. In our study, compound **MH-79** was the most effective in reversing endothelial dysfunction. We showed **MH-79** to have a renoprotective effect, attenuating renal inflammation and fibrosis. **MH-79** was also the most potent in reducing renal tubulointerstitial damage, and it was the only compound able to reduce proinflammatory cell infiltration in the kidney and heart. **MH-79** was also the most effective in reversing renal and coronary atherosclerotic plaque formation and other arteriosclerotic alterations in coronary arteries. We suggest that this is due to the high ability of MH-79 to protect endothelial integrity in addition to α1-adrenoceptor blocking activity, which intensifies its hypotensive effect and reduces the infiltration of inflammatory cells, thus protecting the histoarchitecture of the kidney, heart, and blood vessels. As inflammation and oxidative stress are involved in renal and cardiac injury in the DOCA-salt model, we also studied the effect of **MH-76**, **MH-79**, and prazosin on selected inflammation markers and evaluated their antioxidant activity.

CRP is an inflammation marker that is elevated in hypertensive patients and is associated with target organ

damage [33, 34]. In our study, treatment with all α1-adrenoceptor blockers decreased the elevated CRP concentration. We found that **MH-76** showed significant antioxidant properties and an ability to decrease IL-6 concentration in the kidney, which is in line with our previous research where MH-76 exerted an anti-inflammatory effect (unpublished data); however, in this study, MH-76 was not superior to MH-79, which suggests that the beneficial effect of MH-79 on kidney histopathology is not directly related to inflammatory mediators such as IL-6 or CRP. The obtained results suggest that targeting endothelial integrity and endothelial protection is more beneficial in this particular setting.

The potential proapoptotic and necrotic effect of quinazoline derivatives was a starting point in this study. However, we found only an insignificant intensification of apoptosis in DOCA-salt and DOCA-salt + prazosin-treated rats. However, we revealed the unfavorable effect of prazosin on blood vessels. Treatment with prazosin also resulted in an elevated IL-6 concentration in the kidney, which was even higher in DOCA-salt rats. This finding is in line with results of the study performed by Lin and Chuang [35], who revealed that a high therapeutic concentration of prazosin can upregulate IL-6 genes. To the best of our knowledge, it is shown for the first time that prazosin caused the calcification of coronary arteries and fibrosis of the tunica media in renal arteries. Vascular calcification is prevalent in clinical states characterized by low-grade chronic inflammation; however, the mechanisms of observed alterations need further studies, but we think that they are independent of α1-adrenoceptor blockade, as the studied compounds, **MH-76** and **MH-79**, did not induce such unfavorable effects. Specifically, the calcification is probably the effect evoked by quinazoline-derivative prazosin only, as even DOCA-salt treatment did not induce such mineralization.

In summary, we report the beneficial effect of non-quinazoline α1-adrenolytics on cardiac, vascular and renal dysfunction in DOCA-salt hypertensive rats. The protective effect of these compounds may be attributed to blood pressure reduction through α1-adrenoceptor antagonism, reduction of sympathetic nervous system activity, and decreased vasoconstriction in the coronary and systemic circulation, with favorable consequences on the heart and kidney structure. Moreover, the studied compounds, especially **MH-79**, reversed endothelial dysfunction, which reduced inflammatory cell infiltration, arteriosclerotic alterations in renal and coronary arteries, and reduced tubulointerstitial fibrosis. Prazosin, despite strong blood-pressure-lowering activity and its associated benefits, revealed detrimental effects on coronary and renal arteries. Prazosin did not reverse endothelial dysfunction. Our results showed that α1-blockade cannot be definitely

excluded from the treatment of hypertension and may be considered an important part of a multidirectional approach to the pharmacotherapy of cardiovascular diseases. Our results also support the idea that targeting endothelial protection and endothelial integrity would exert beneficial effects against cardiac, vessels, and renal injury related to hypertension.

Compliance with ethical standards

Publisher's note: Springer Nature remains neutral with regard to jurisdictional claims in published maps and institutional affiliations.

References

1. Pessina AC, Ciccariello L, Perrone F, Stoico V, Gussoni G, Scotti A, et al. Clinical efficacy and tolerability of alpha-blocker doxazosin as add-on therapy in patients with hypertension and impaired glucose metabolism. Nutr Metab Cardiovasc Dis. 2006;16:137–47.
2. Basting T, Lazartigues E. DOCA-salt hypertension: an update. Curr Hypertens Rep. 2017;19:32.
3. Chapman N, Chen CY, Fujita T, Hobbs FD, Kim SJ, Staessen JA, et al. Time to re-appraise the role of alpha-1 adrenoceptor antagonists in the management of hypertension? J Hypertens. 2010;28:1796–803.
4. Eiras S, Fernández P, Piñeiro R, Iglesias MJ, González-Juanatey JR, Lago F. Doxazosin induces activation of GADD153 and cleavage of focal adhesion kinase in cardiomyocytes en route to apoptosis. Cardiovasc Res. 2006;71:118–28.
5. Chapman N, Chang CL, Dahlöf B, Sever PS, Wedel H, Poulter NR.ASCOT Investigators. Effect of doxazosin gastrointestinal therapeutic system as third-line antihypertensive therapy on blood pressure and lipids in the Anglo-Scandinavian cardiac outcomes trial. Circulation. 2008;118:42–8.
6. Qian X, Li M, Wagner MB, Chen G, Song X. Doxazosin stimulates galectin-3 expression and collagen synthesis in HL-1 cardiomyocytes independent of protein kinase C pathway. Front Pharmacol. 2016;20:495.
7. Kyprianou N, Vaughan TB, Michel MC. Apoptosis induction by doxazosin and other quinazoline alpha1-adrenoceptor antagonists: a new mechanism for cancer treatment? Naunyn Schmiede Arch Pharmacol. 2009;380:473–7.
8. Tahmatzopoulos A, Kyprianou N. Apoptotic impact of alpha1-blockers on prostate cancer growth: a myth or an inviting reality? Prostate. 2004;59:91–100.
9. Bilbro J, Mart M, Kyprianou N. Therapeutic value of quinazoline-based compounds in prostate cancer. Anticancer Res. 2013;33:4695–700.
10. González-Juanatey JR, Iglesias MJ, Alcaide C, Piñeiro R, Lago F. Doxazosin induces apoptosis in cardiomyocytes cultured in vitro by a mechanism that is independent of alpha1-adrenergic blockade. Circulation. 2003;107:127–31.
11. Marona H, Kubacka M, Filipek B, Siwek A, Dybała M, Szneler E, et al. Synthesis, alpha-adrenoceptors affinity and alpha 1-adrenoceptor antagonistic properties of some 1,4-substituted piperazine derivatives. Pharmazie. 2011;66:733–9.
12. Kubacka M, Mogilski S, Filipek B, Marona H. The hypotensive activity and alpha1-adrenoceptor antagonistic properties of some aroxyalkyl derivatives of 2-methoxyphenylpiperazine. Eur J Pharmacol. 2013;698:335–44.
13. Kubacka M, Kotańska M, Kazek G, Waszkielewicz AM, Marona H, Filipek B, et al. Involvement of the NO/sGC/cGMP/K + channels pathway in vascular relaxation evoked by two non-quinazoline α1-adrenoceptor antagonists. Biomed Pharmacother. 2018;103:157–66.
14. Bae EH, Kim IJ, Park JW, Ma SK, Lee JU, Kim SW. Renoprotective effect of rosuvastatin in DOCA-salt hypertensive rats. Nephrol Dial Transplant. 2010;25:1051–9.
15. Iyer A, Chan V, Brown L. The DOCA-salt hypertensive rat as a model of cardiovascular oxidative and inflammatory stress. Curr Cardiol Rev. 2010;6:291–7.
16. Sharma B, Singh N. Experimental hypertension induced vascular dementia: pharmacological, biochemical and behavioral recuperation by angiotensin receptor blocker and acetylcholinesterase inhibitor. Pharmacol Biochem Behav. 2012;102:101–8.
17. Dudek M, Bednarski M, Bilska A, Iciek M, Sokołowska-Jezewicz M, Filipek B, et al. The role of lipoic acid in prevention of nitroglycerin tolerance. Eur J Pharmacol. 2008;591:203–10.
18. Sedlak J, Lindsay RH. Estimation of total, protein-bound and non-protein sulfhydryl groups in tissue with Ellman's reagent. Anal Biochem. 1968;25:192–205.
19. Guillaume P, Provost D, Legrand P, Godes M, Lacroix P. Models of cardiovascular disease: measurement of antihypertensive activity in the conscious rat (SHR, DOCA-salt, and Goldblatt hypertension models). Curr Protoc Pharmacol. 2009;5:53.
20. Toba H, Yoshida M, Tojo C, Nakano A, Oshima Y, Kojima Y, et al. L/N-type calcium channel blocker cilnidipine ameliorates proteinuria and inhibits the renal renin-angiotensin-aldosterone system in deoxycorticosterone acetate-salt hypertensive rats. Hypertens Res. 2011;34:521–9.
21. Perlini S, Palladini G, Ferrero I, Tozzi R, Fallarini S, Facoetti A, et al. Sympathectomy or doxazosin, but not propranolol, blunt myocardial interstitial fibrosis in pressure-overload hypertrophy. Hypertension. 2005;46:1213–8.
22. Kubacka M, Mogilski S, Bednarski M, Nowiński L, Dudek M, Żmudzka E, et al. Antidepressant-like activity of aroxyalkyl derivatives of 2-methoxyphenylpiperazine and evidence for the involvement of serotonin receptor subtypes in their mechanism of action. Pharmacol Biochem Behav. 2016;141:28–41.
23. Dooley M, Goa KL. Urapidil. A reappraisal of its use in the management of hypertension. Drugs. 1998;56:929–55.
24. Kolassa N, Beller KD, Sanders KH. Involvement of brain 5-HT1A receptors in the hypotensive response to urapidil. Am J Cardiol. 1989;64:7D–10D.
25. Van Zwieten PA, Blauw GJ, van Brummelen P. Pharmacological profile of antihypertensive drugs with serotonin receptor and alpha-adrenoceptor activity. Drugs. 1990;40(Suppl. 4):1–8.
26. Gandhi H, Naik P, Agrawal N, Yadav M. Protective effects of MCR-1329, a dual α1 and angII receptor antagonist, in mineralocorticoid-induced hypertension. Pharmacol Rep. 2016;68:952–9.
27. Bae EH, Kim IJ, Joo SY, Kim EY, Kim CS, Choi JS, et al. Renoprotective effects of sildenafil in DOCA-salt hypertensive rats. Kidney Blood Press Res. 2012;36:248–57.
28. Pawluczyk IZ, Patel SR, Harris KP. The role of the alpha-1 adrenoceptor in modulating human mesangial cell matrix production. Nephrol Dial Transplant. 2006;21:2417–24.
29. Chistiakov DA, Orekhov AN, Bobryshev YV. Endothelial barrier and its abnormalities in cardiovascular disease. Front Physiol. 2015;9:365.

30. Hirase T, Node K. Endothelial dysfunction as a cellular mechanism for vascular failure. Am J Physiol Heart Circ Physiol. 2012;302:H499–H505.

31. Ter Maaten JM, Damman K, Verhaar MC, Paulus WJ, Duncker DJ, Cheng C, et al. Connecting heart failure with preserved ejection fraction and renal dysfunction: the role of endothelial dysfunction and inflammation. Eur J Heart Fail. 2016;18:588–98.

32. Du YH, Guan YY, Alp NJ, Channon KM, Chen AF. Endothelium-specific GTP cyclohydrolase I overexpression attenuates blood pressure progression in salt-sensitive low-renin hypertension. Circulation. 2008;117:1045–54.

33. Dinh QN, Drummond GR, Sobey CG, Chrissobolis S. Roles of inflammation, oxidative stress, and vascular dysfunction in hypertension. Biomed Res Int. 2014;2014:406960.

34. Tsounis D, Bouras G, Giannopoulos G, Papadimitriou C, Alexopoulos D, Deftereos S. Inflammation markers in essential hypertension. Med Chem. 2014;10:672–81.

35. Lin ZY, Chuang WL. High therapeutic concentration of prazosin up-regulates angiogenic IL6 and CCL2 genes in hepatocellular carcinoma cells. Biomed Pharmacother. 2012;66:583–6.